

## A Hot Wind from the Classical T Tauri Stars: TW Hydrae and T Tauri

A. K. Dupree<sup>1,2,3</sup>, N. S. Brickhouse<sup>1,3</sup>

and

Graeme H. Smith<sup>4</sup> and Jay Strader<sup>4</sup>

### ABSTRACT

Spectroscopy of the infrared He I ( $\lambda 10830$ ) line with KECK/NIRSPEC and IRTF/CSHELL and of the ultraviolet C III ( $\lambda 977$ ) and O VI ( $\lambda 1032$ ) emission with *FUSE* reveals that the classical T Tauri star TW Hydrae exhibits P Cygni profiles, line asymmetries, and absorption indicative of a continuous, fast ( $\sim 400$  km/s), hot ( $\sim 300,000$  K) accelerating outflow with a mass loss rate  $\sim 10^{-11}$ – $10^{-12}$   $M_{\odot} \text{ yr}^{-1}$  or larger. Spectra of T Tauri N appear consistent with such a wind. The source of the emission and outflow seems restricted to the stars themselves. Although the mass accretion rate is an order of magnitude less for TW Hya than for T Tau, the outflow reaches higher velocities at chromospheric temperatures in TW Hya. Winds from young stellar objects may be substantially hotter and faster than previously thought.

*Subject headings:* stars:pre-main sequence stars: winds, outflows stars: individual (TW Hya, T Tau) infrared: stars ultraviolet: stars

---

<sup>1</sup>Harvard-Smithsonian Center for Astrophysics, Cambridge MA 02138; adupree@cfa.harvard.edu, nbrickhouse@cfa.harvard.edu

<sup>2</sup>Visiting Astronomer at the Infrared Telescope Facility, which is operated by the University of Hawaii under Cooperative Agreement no. NCC5-538 with the National Aeronautics and Space Administration, Office of Space Science, Planetary Astronomy Program.

<sup>3</sup>Guest Investigator, Far Ultraviolet Spectroscopic Explorer— a NASA-CNES-CSA FUSE mission operated by the Johns Hopkins University; Based in part on data from the MAST Archive.

<sup>4</sup>University of California Observatories/Lick Observatory, Department of Astronomy & Astrophysics, University of California, Santa Cruz CA 95064; graeme@helios.ucsc.edu, strader@ucolick.org

## 1. Introduction

Young stars with accretion disks display energetic jets observed in optical transitions from low stages of ionization: [O I], [Fe II], [S II], [N I], [N II], as well as molecular outflows. The source of these outflows is not well determined. Shu et al. (1994) argue they arise from the truncation region of the accretion disk where the stellar magnetosphere, frozen into the disk, causes super-Keplerian rotation and drives a magnetocentrifugally accelerated wind. Königl & Pudritz (2000) suggest an extended region of the accretion disk itself may be responsible. Or, several regions may contribute to a cool wind as indicated by [Fe II]: the disk forming a wide angle low velocity component, whereas a high velocity component is launched from a region next to the truncation radius (Pyo et al. 2003). In addition, near UV and optical lines show signs of outflow apparently from the photosphere and low chromosphere (Ardila et al. 2002; Herczeg et al. 2002). To date, the dynamics and energetics of the outflows in young stars have been principally constrained by these low temperature species and the modeled winds are generally cool,  $T < 10^4\text{K}$  (Shang et al. 2002). Beristain et al. (2001) detected broad wings in He I 5876Å, and suggested this signaled a warmer wind. It is important to determine physical properties of these winds and identify their source for they can affect angular momentum loss, disk structure, and acceleration of optical jets.

Additional unique spectral features can provide diagnostics of the dynamics of outflows from young stars and are reported here. Two transitions are particularly valuable: the chromospheric He I ( $\lambda 10830$ ;  $2s\ ^3S \rightarrow 2p\ ^3P^0$ ) line arising from a metastable state predominantly populated by recombination following photoionization by the euv continuum. In a cool luminous star, this transition is generally formed higher in the atmosphere ( $T \sim 20000\text{K}$ ) than H $\alpha$  and the Ca II and Mg II emission cores (Dupree et al. 1992). Because  $\lambda 10830$  is not coupled to local conditions, it is useful to indicate bulk motions in cool stars including a handful of young stellar objects (Dupree et al. 1992; Edwards et al. 2003; Takami et al. 2002; Dupree 2004). Importantly, this He I line is unaffected by interstellar or circumstellar absorption. Another valuable diagnostic is the resonance line of C III ( $\lambda 977$ ), which has the highest opacity of any of the major ultraviolet resonance transitions. Judged by atomic physics, the opacity of C III  $\lambda 977$  exceeds all other major far-uv resonance lines by factors of 3 to 10 (Dupree et al. 2005), making it sensitive to absorption that could reveal the presence of a wind. In a collisionally ionized plasma C III signals temperatures  $\sim 80,000\text{K}$  (Young et al. 2003). Effects of mass motions causing asymmetries in ultraviolet line profiles are widely observed in luminous cool stars (Dupree & Brickhouse 1998, Carpenter et al. 1999, Dupree et al. 2005) and the interpretation of asymmetries in relation to atmospheric dynamics is confirmed from semi-empirical modeling (Lobel & Dupree 2001).

Two well-studied classical T Tauri stars are good targets. TW Hydrae and T Tauri

have rotation axes oriented with low inclinations,  $<20^\circ$ , and between  $8$  and  $13^\circ$  respectively (Krist et al. 2000; Herbst et al. 1986) so that the stellar polar regions are observed directly. The accretion disks are observed face-on. Although the dipole component of the stellar magnetic field, where disk material is thought to be channeled to the star and thermalized in an accretion shock (Hartmann 1998 and references therein) may not be aligned with the rotation axis of the star, it is still in view. TW Hya is older (10 Myr), than T Tau, and the accretion rate may be low [ $\sim 4 \times 10^{-10} M_\odot \text{ yr}^{-1}$ , from H- $\alpha$ , (Muzerolle et al. 2000) to  $10^{-8}$ – $10^{-9} M_\odot \text{ yr}^{-1}$  from Na D (Alencar & Batalha 2002)] whereas T Tau N, (7.3 Myr) has a much higher accretion rate of  $3.1$ – $5.7 \times 10^{-8} M_\odot \text{ yr}^{-1}$  to  $3 \times 10^{-7} M_\odot \text{ yr}^{-1}$  (Calvet et al. 2004; Johns-Krull et al. 2000). Since mass outflows are thought to be proportional to the mass accretion rate (Calvet 2004), different winds might be expected from these 2 stars.

## 2. Observations

TW Hya was observed at He I  $\lambda 10830$  in July 2002 at KECK II<sup>1</sup> using the NIRSPEC instrument (McLean et al. 1998). Observations were made using the echelle cross-dispersed mode with the NIRSPEC-1 order-sorting filter and a slit of  $0.43 \times 12$  arcsec, yielding a nominal resolving power of 23,600. Fringing was minimized by not using the two PK50 blocking glass filters. The exposure time totaled 480 seconds. The spectrum was reduced using the REDSPEC IDL software package. The wavelength scale was established using NeArKr arc lamps and is set to photospheric values using the Si I and Mg I absorption as reference. He I  $\lambda 10830$  in T Tau was observed at the IRTF with CSHELL (Greene et al. 1993) in Aug. 1992. A 1 arcsec slit was used; the instrumental resolution is  $15 \text{ km s}^{-1}$ , and the exposure time was 10 minutes. This spectrum shows residual fringing near  $-400 \text{ km s}^{-1}$ . Standard IRAF procedures were used to reduce the spectra. The wavelength scale, determined by Ar and Kr lamps, is set to the photospheric value, using the Si I absorption at  $\lambda 10844.02$ . Figs. 1 and 2 show that both stars have He I P Cygni profiles. The absorption extent reaches  $-280 \text{ km s}^{-1}$  in TW Hya, and  $-220 \text{ km s}^{-1}$  in T Tau. Since the He I line is formed at chromospheric temperatures, these velocities are supersonic and may be an indication of shocks and transient events. The photospheric escape velocity is  $\sim 500 \text{ km s}^{-1}$

---

<sup>1</sup>Data were obtained at the W. M. Keck Observatory, which is operated as a scientific partnership among the California Institute of Technology, the University of California, and the National Aeronautics and Space Administration. The Observatory was made possible by the generous financial support of the W. M. Keck Foundation. The authors recognize and acknowledge the very significant cultural role and reverence that the summit of Mauna Kea has always had within the indigenous Hawaiian community. We are most fortunate to have the opportunity to conduct observations from this mountain.

for these stars, but at a distance of  $1R_{\star}$  above the surface, the escape speed approaches  $300 \text{ km s}^{-1}$  so a small extension of the atmosphere could easily lead to mass loss.

*FUSE* spectra (Moos et al. 2000) of TW Hya (Fig. 1), obtained from the MAST archive, have a total exposure time of 30.6 ks. Exposure set C0670101 (15.9 ks) was centered at JD 2452690.834; exposure set C0670102 (14.7 ks) was taken one day later. We use the total exposure. Segments of the SiC2A exposures were examined to insure that the channel alignment was in place; segment 1 of C0670102 was discarded because of the short exposure time. Extractions of night-only observations were made using CALFUSE 2.4 to verify that scattered solar light is absent in the day spectra. Individual segments were cross correlated using stellar emission lines and summed for SiC2A (containing  $977\text{\AA}$ ) and LiF1A (containing  $1032\text{\AA}$ ). The wavelength offsets are determined using interstellar absorption features in the spectrum. For TW Hya, interstellar absorption of O I, C II, Si II and Mg II occurs at a heliocentric velocity of  $0\pm 3 \text{ km s}^{-1}$  (Herczeg et al. 2004), and the interstellar absorption in the C III  $\lambda 977$  line has been set to that velocity with an uncertainty of about  $\pm 5 \text{ km s}^{-1}$ . The radial velocity of TW Hya is taken as  $+12.5 \text{ km s}^{-1}$  (Alencar & Batalha 2002). The wavelength offset for the LiF1A channel was adopted from the CALFUSE reduction. Since that channel is used for *FUSE* guiding, the offset is the most reliable; the observed wavelengths of the airglow lines are equal to their rest values within a few  $\text{km s}^{-1}$ , giving support to this offset. The uncertainty in this procedure is about  $\pm 10 \text{ km s}^{-1}$ . Far UV spectra of T Tau N were obtained from the *FUSE* archive (P1630101) where reduction procedures similar to those described above were followed. The shortest exposure segments were deleted from 14 data segments to achieve a total exposure of 19.5 ks. Interstellar lines observed in Mg II at  $+8 \text{ km s}^{-1}$  (Ardila et al. 2002) set the SiC2A scale by matching to the interstellar C III absorption. The radial velocity of T Tau is taken as  $+17.5 \text{ km s}^{-1}$ .

### 3. Evidence for Hot Winds

The profile of C III ( $\lambda 977$ ) in TW Hya exhibits P Cygni structure with a clear absorption trough recovering near  $-325 \text{ km s}^{-1}$  and extending to higher outflow velocities than the He I line. As expected (Hummer & Rybicki 1968; Lobel & Dupree 2001), a self-absorbed line in a differentially expanding atmosphere, appears asymmetric with a steeper slope occurring on the negative velocity side than on the positive velocity side of the profile. A similar shape is found in the O VI line, although no diminution of absorption creating an emission ‘bump’ is detected. Since cool stars lack a local continuum in this part of the far uv spectrum, the line intensity drops to near zero, exactly what is observed in C III and O VI. The similarity of the profile shapes in TW Hya suggests that the wind at the C III level (80,000K) continues

to higher temperatures of  $3 \times 10^5 \text{K}$  (Young et al. 2003), indicated by the presence of O VI asymmetry, assuming a collisionally ionized plasma. The C IV and N V profiles of TW Hya (Herczeg et al. 2002) also show the same asymmetry as O VI, typical of wind absorption.

The presence of wind opacity can be investigated by fitting a Gaussian profile to the long wavelength wing of the UV lines in TW Hya (Fig. 1). These one-sided fits predict line centers of  $-13 \pm 5$  and  $+3 \pm 9 \text{ km s}^{-1}$  for C III and O VI respectively and have similar FWHM (C III:  $1.04 \pm 0.02 \text{ \AA}$ , and O VI:  $1.14 \pm 0.04 \text{ \AA}$ ). The difference between the observed profile and the fit reveals the wind absorption. In Fig. 3, the profiles are normalized to the local continuum provided by the Gaussian fit. The furthest outward extent of the profile reaches  $-260 \text{ km s}^{-1}$  for He I,  $-325 \text{ km s}^{-1}$  for C III, and  $-440 \text{ km s}^{-1}$  for O VI. These values are in harmony with the velocity of cooler material inferred from HST/STIS spectra to be  $-230 \text{ km s}^{-1}$  from lines of O I, C II, and N I (Herczeg et al. 2002) suggesting the accelerating outflow typical of a stellar wind. Solar wind models (Hu et al. 2000) demonstrate that ions possess different speeds depending on mass, charge, and wind heating characteristics.

A rough estimate of the mass loss rate required to produce the absorption profiles in Fig. 3 can be derived from the Sobolev optical depth, assuming  $\tau_{\text{Sobolev}}=1$  (Hartmann 1998). For an outflow velocity of  $400 \text{ km s}^{-1}$  (the total width of the O VI absorption), reached over a distance of  $R_{\text{star}}$ , and a solar oxygen abundance ( $\text{O}/\text{H}=8.5 \times 10^{-4}$ ) with maximum fractional ionization for O VI of 0.2, the mass loss rate follows as:  $\dot{M}_{\text{O VI}}/\phi = 2.3 \times 10^{-11} (M_{\odot} \text{ yr}^{-1})$  where  $\phi$  is the fraction of the surface where the wind originates. Similarly for C III, an acceleration to  $300 \text{ km s}^{-1}$ , over  $R_{\text{star}}$  suggests  $\dot{M}_{\text{C III}}/\phi = 1.3 \times 10^{-12} (M_{\odot} \text{ yr}^{-1})$ , taking  $\text{C}/\text{H}=3.6 \times 10^{-4}$  and a fractional ionization of 0.8. A wind from high latitude regions might have  $\phi \sim 0.3$ . These values are less than the accretion rate inferred from H- $\alpha$ ,  $4 \times 10^{-10} M_{\odot} \text{ yr}^{-1}$  (Muzerolle et al. 2000). However, if wind optical depths are much larger, possibly  $10^3$  (Hartmann 1998), the mass loss rate becomes comparable to the accretion rate.

The far UV spectrum of T Tau is clearly of lesser quality than that of TW Hya, but characteristics of the profiles are similar to TW Hya: namely, a P Cygni He I line extending to  $-220 \text{ km s}^{-1}$ , a C III width less than O VI, and profiles consistent with blue asymmetry. In T Tau, the far UV lines are narrower than the He I emission which, in a wind model, would suggest absorption with higher column density than in TW Hya.

#### 4. Discussion and Conclusions

It is difficult to determine the source of the UV line emission that provides the flux for wind scattering, but it must be close to the star. Dwarf stars show strong emission

from C III and O VI (Redfield et al. 2002) associated with activity, and we expect a similar contribution here. UV line fluxes generally increase in T Tauri stars which are undergoing accretion, suggesting an origin in the accretion disk, X-region, or the shocked accretion column. The accretion disks in both sources contain H<sub>2</sub>, are dusty, and thus are unlikely to create and support plasma at 10<sup>5</sup> K. The intersection of the dipole magnetic field from the star and the accretion disk, perhaps the source of the X-wind, is also unlikely to be responsible as it is thought to be ionized and heated by X-rays only to temperatures of  $\sim 10^4$  K or less (Shang et al. 2002). Part of the UV emission undoubtedly results from the accretion shock. Profiles of emission from highly ionized ions in an accretion shock have not been reliably calculated; the emission observed might arise either from turbulent broadening associated with the shocked, cooling gas, or from infalling gas from the near-side accretion stream. Non-thermal broadening could produce intrinsically symmetric profiles as modeled here. On the other hand, emission from the infalling gas on the far-side might be blocked by the star, producing an intrinsically asymmetric profile. The emission at  $-320 \text{ km s}^{-1}$  in the C III line seems to rule out this second case, as we would expect similar features from C IV, N V, and O VI. Furthermore, the star would preferentially block the highest velocities, not the lowest velocities, since the accretion stream accelerates toward the stellar surface.

T Tauri stars are frequently associated with optical jets and Herbig-Haro (HH) objects. Because our targets are face on, jets along the line of sight might contribute emission from high temperature material. However, high excitation HH objects that contain C IV also exhibit a UV continuum (Bohm et al. 1987) that is absent here. One of the brightest HH objects in the sky shows neither C III nor O VI in a *Hopkins Ultraviolet Telescope* spectrum (Raymond et al. 1997). FUSE spectra of HH1 and HH2 obtained from the MAST archive, also give no signs of these ions. Thus it is not likely that HH objects contribute to the emission reported here.

The emission components of C III and O VI are exceptionally broad. Both T Tau and TW Hya are slow rotators [ $v \sin i = 20.9$  and  $5 \pm 2 \text{ km s}^{-1}$ , respectively (Hartmann et al. 1986; Alencar & Batalha 2002)], yet the observed emission line widths exceed those values (C III:  $102 \text{ km s}^{-1}$  and  $202 \text{ km s}^{-1}$ ; O VI:  $140 \text{ km s}^{-1}$  and  $219 \text{ km s}^{-1}$  respectively). Accounting for absorption can nearly double the intrinsic widths. If the emission is attributed to active regions, the broadening would represent an extreme example of the weak broadening found in normal stars (Redfield et al. 2002). Emission associated with the accretion flow and shock is likely to show turbulent broadening. We note that the UV line widths are significantly larger than the X-ray line widths. If the X-rays from TW Hya are generated at the accretion shock (Kastner et al. 2002), the UV lines may not be directly associated with the shock. On the other hand, studies of X-ray emission in young star clusters, suggest that the strength of the X-ray emission is correlated with stellar rotation, thus casting doubt on an accretion

origin for the X-rays (Stassun et al. 2004).

Whatever the source of these collisionally excited photons, originating on or close to the star, they appear to be scattered in the outflowing plasma, producing a sequence of similar P Cygni profiles ranging from He I and C III to O VI. In our interpretation, the wind signatures indicate a continuous outward acceleration from approximately the photospheric velocity to several hundred  $\text{km s}^{-1}$ , and reach temperatures of  $3 \times 10^5$  K. A cool wind has been suggested in TW Hya (Herczeg et al. 2002, 2004) as a component in the complex Lyman- $\alpha$  profile, and also from the weakness of one  $\text{H}_2$  line possibly affected by C II absorption. Other  $\text{H}_2$  transitions subject to wind absorption may offer insight into the configuration of the stellar wind if the site of the fluoresced  $\text{H}_2$  can be identified. A high temperature, fast wind might contribute to the opacity needed (Stassun et al. 2004) for the absorption of X-rays in accreting systems. In addition, a fast hot wind may influence the diminution of dust in accretion disks (Alexander et al. 2005).

Detailed semi-empirical modeling will be necessary to derive meaningful mass loss rates. The velocities observed in TW Hya are larger than in T Tau, although the wind may be less opaque, which is surprising if wind characteristics are related to the accretion rate.

The profiles reported here are consistent with the presence of hot winds reaching escape velocities, that may lead to shocks and optical jets as the wind decelerates at greater distances from the star. The polar orientation of TW Hya and T Tau enabled full access to regions likely to contain open field lines enhancing mass outflow. Observations of disk-star systems at various inclination angles can help to define the structure of both the emission region and the wind.

We wish to thank Ian McLean and the NIRSPEC team for both the development of this instrument and the REDSPEC reduction software. We also thank Lee Hartmann for useful discussions. J.S. acknowledges support from an NSF Graduate Research Fellowship.

## REFERENCES

- Alencar, S. H. P., & Batalha, C. 2002, *AJ*, 571, 378
- Alexander, R. D., Clarke, C. J., & Pringle, J. E. 2005, *MNRAS*, 358, 283
- Ardila, D. R., Basri, G., Walter, F. M., Valenti, J. A., & Johns-Krull, C. M. 2002, *ApJ*, 567, 1013
- Beristain, G., Edwards, S., & Kwan, J. 2001, *ApJ*, 551, 1037

- Böhm, K. H., Bührke, T. Raga, A. C., Brugel, E. W., Witt, A. N., & Mundt, R. 1987, *ApJ*, 316, 349
- Carpenter, K. G., Robinson, R. D., Harper, G. M., Bennett, P. D., Brown, A., & Mullan, D. J. 1999, *ApJ*, 521, 382
- Calvet, N. 2004, in *Stars as Suns: Activity, Evolution and Planets*, IAU Sym 219, ed. A. K. Dupree & A. O. Benz, 599
- Calvet, N., Muzerolle, J., Briceño, Hernández, J., Hartmann, L., Saucedo, J. L. & Gordon, K. D. 2004, *AJ*, 128, 1294
- Dupree, A. K. 2004, *Stars as Suns: Activity, Evolution, and Planets*, IAU Symp. Vol. 219, ed A. K. Dupree & A. O. Benz, 623
- Dupree, A. K., & Brickhouse, N. S. 1998, *ApJ*, 500, L33
- Dupree, A. K., Lobel, A., Young, P. R., Ake, T. B., Linsky, J. L., & Redfield, S. 2005, *ApJ*, 622, 629
- Dupree, A. K., Sasselov, D. D., & Lester, J. B. 1992, *ApJ*, 387, L85
- Edwards, S., Fischer, W., Kwan, J., Hillenbrand, L., & Dupree, A. K., 2003, *ApJ*, 599, L41
- Greene, T. P., Tokunaga, A. T., Toomey, D. W., & Carr, J. S. 1993, *Proc, SPIE*, 1946, 313
- Hartmann, L. 1998, *Accretion Processes in Star Formation*, Cambridge: Cambridge Univ. Press
- Hartmann, L., Hewett, R., Stahler, S., & Mathieu, R. D. 1986, *ApJ*, 309, 275
- Herbst, W., et al. 1986, *ApJ*, 310, L71
- Herczeg, G. J., Linsky, J. L., Valenti, J. A., Johns-Krull, C. M., & Wood, B. E. 2002, *ApJ*, 572, 310
- Herczeg, G. J., Wood, B. E., Linsky, J. L., Valenti, J. A., & Johns-Krull, C. M. 2004, *ApJ*, 607, 369
- Hu, Y. Q., Esser, R., & Habbal, S. R. 2000, *JGR*, 105, A3, 5093
- Hummer, D. G., & Rybicki, G. B. 1968, *ApJ*, 153, L107
- Johns-Krull, C. M., Valenti, J. A., & Linsky, J. L. 2000, *ApJ*, 539, 815



- Kastner, J. H., Huenemoerder, D. P., Schulz, N. S., Canizares, C. R., & Weintraub, D. A. 2002, *ApJ*, 567, 434
- Königl, A., & Pudritz, R. E. 2000, in *Protostars and Planets IV*, ed V. Mannings, A. P. Boss, & S. S. Russell, (Tucson: U of AZ Press), 759
- Krist, J. E., Stapelfeldt, K. R., Ménard, F., Padgett, D. L. & Burrows, C. J. 2000, *ApJ*, 538, 793
- Lobel, A., & Dupree, A. K. 2001, *ApJ*, 558, 815
- McLean, I. S., et al. 1998, *Proc. SPIE*, 3354, 566
- Moos, H. W., et al. 2000, *ApJ*, 538, L1
- Muzerolle, J., Calvet, N., Briceño, C., Hartmann, L., & Hillenbrand, L. 2000, *ApJ*, 535, L47
- Pyo, T.-S., et al. 2003, *ApJ*, 590, 340
- Raymond, J. C., Blair, W. P., & Long, K. S. 1997, *ApJ*, 489, 314
- Redfield, S., Linsky, J. L., Ake, T. B., Ayres, T. R., Dupree, A. K., Robinson, R. D., Wood, B. E., & Young, P. B. 2002, *ApJ*, 581, 626
- Shang, H., Glassgold, A. E., Shu, F. H., & Lizano, S. 2002, *ApJ*, 564, 853
- Shu, F., Najita, J., Ostriker, E., Wilkin, F., Ruden, S., & Lizano, S. 1994, *ApJ*, 429, 781
- Stassun, K. G., Ardila, D. R., Barsony, M, Basri, G., & Mathieu, R. D. 2004, *AJ*, 127, 3537
- Takami, M., Chrysostomou, A., Bailey, J., Gledhill, T., Tamura, M., & Terada, H. 2002, *ApJ*, 568, L53
- Walter, F., et al. 2003, *AJ*, 126, 3076
- Young, P. R., DelZanna, G. Landi, E., Dere, K. P., Mason, H. E., & Landini, M. 2003, *ApJS*, 144, 135

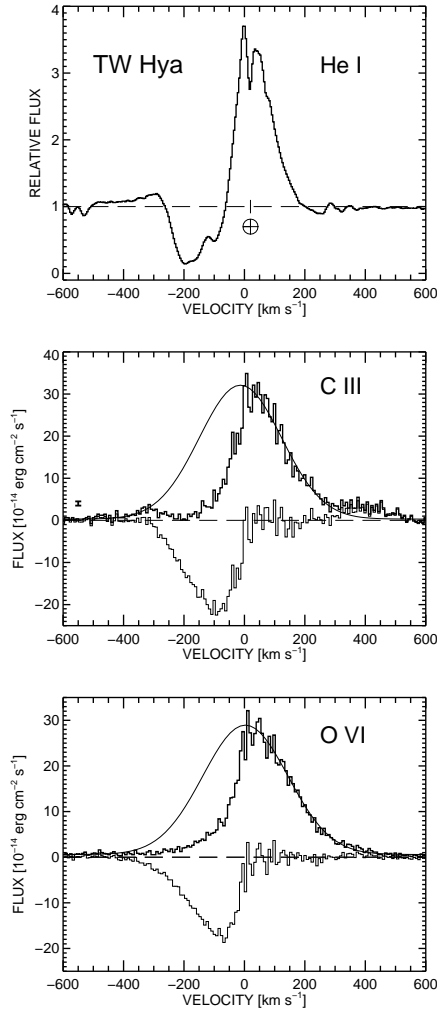


Fig. 1.— He I  $\lambda 10830$ , C III  $\lambda 977$ , and O VI  $\lambda 1032$  transitions in TW Hya. The notch in the TW Hya spectrum of He I at  $-100 \text{ km s}^{-1}$  is found also at times in H- $\alpha$  profiles (Alencar & Batalha 2002). The ultraviolet line profiles have been fit on the positive velocity side by a gaussian profile. The difference between the observed profile and the gaussian fit is shown below the original spectrum. Extraction of the spectra taken during the *FUSE* night, demonstrates that the low level emission near C III centered at  $-320 \text{ km s}^{-1}$  and  $+400 \text{ km s}^{-1}$  is associated with the star, and is not contaminated by airglow emission. The emission feature at  $-320 \text{ km s}^{-1}$  in the C III profile has a  $6\sigma$  significance in one bin sampled twice per resolution element. Emission present at  $+400 \text{ km s}^{-1}$  in the C III profile, might originate from the star itself (although a full extent of the line to  $\pm 500 \text{ km s}^{-1}$  may be excessive) or it could be due to O I ( $\lambda 978.624$ ) that is fluoresced by the stellar C III line, and arising in the expanding wind with an outflow of  $\sim 100 \text{ km s}^{-1}$ . A similar feature is identified in the *FUSE* spectrum of the cool supergiant  $\beta$  Dra (Dupree et al. 2005).

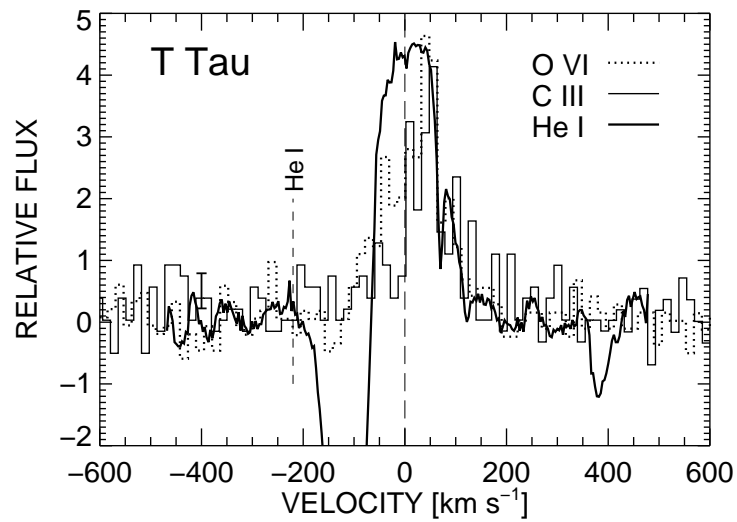


Fig. 2.— He I, C III, and O VI in T Tauri. FUSE spectra are binned to a resolution element. The short dashed line marks the maximum outflow velocity in the He I line at  $-220 \text{ km s}^{-1}$ . Fluoresced  $\text{H}_2$  emission surrounds T Tau (Walter et al. 2003), and there may be narrow absorption in the C III profile,  $-144 \text{ km s}^{-1}$  and  $+370 \text{ km s}^{-1}$  if at the radial velocity of the star. The presence of weak airglow emission in the region between  $-100$  and  $-200 \text{ km s}^{-1}$  in the C III profile can not be excluded.

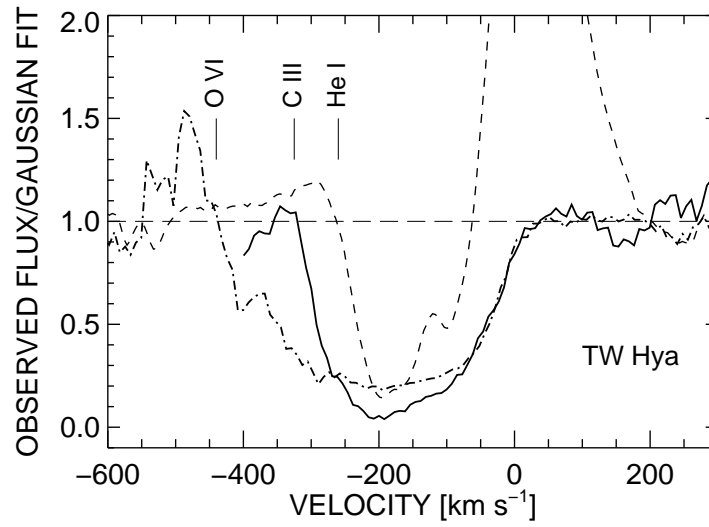


Fig. 3.— Absorption apparent in He I  $\lambda 10830$  (*dashed curve*), C III  $\lambda 977$  (*solid curve*), and O VI  $\lambda 1032$  (*dash-dot curve*) lines in TW Hya. The C III and O VI absorption features are constructed by using the gaussian fit (Fig. 1) as the local continuum and calculating the ratio: Observed Flux/Fit. The He I line is simply the observed profile. The maximum velocity extents of O VI, C III, and He I are marked by vertical lines.